

## Dissipation in a one-dimensional superconductor: Evidence for macroscopic quantum tunneling

N. Giordano

*Department of Physics, Purdue University, West Lafayette, Indiana 47907*

(Received 24 July 1989)

The results of a study of the superconducting transition in very-small-diameter In wires are presented. Several different types of measurements have been performed. First, we have studied the resistive transition in the limit of low applied currents, i.e.,  $I \ll I_c$ , where  $I_c$  is the critical current. Second, the transition to the dissipative state as a function of  $I$  has been examined. The results are discussed initially in terms of the thermal-activation model, according to which the dissipation is due to thermally activated motion of the Ginzburg-Landau order parameter over the free-energy barrier which separates metastable states. For certain ranges of sample size, temperature, and current, the thermal-activation theory is consistent with our results. However, for a wide range of these parameters we find that this theory fails, as the observed transition rates are much larger, and have a qualitatively different temperature dependence, than those predicted by the thermal-activation model. We suggest that in addition to thermal activation, quantum-mechanical tunneling of the order parameter *through* the free-energy barrier may also take place. We show that our results are consistent with this picture.

### I. INTRODUCTION

The present understanding of dissipation in one dimensional superconductors at temperatures  $T \lesssim T_c$  is based largely on the work of Little,<sup>1</sup> Langer and Ambegaokar (LA),<sup>2</sup> and McCumber and Halperin (MH).<sup>3</sup> According to this picture, a current-carrying state is metastable, and dissipation occurs when the system passes, via thermal activation, over the associated free-energy barrier to a state of lower free energy. This process is known as "phase slip," since it involves the time evolution of the phase of the superconducting order parameter. When the current  $I$  is much less than the critical current  $I_c$  and  $T \ll T_c$ , the rate of phase slippage, and hence the dissipation, is negligibly small. However, when one approaches  $T_c$  or  $I_c$ , this rate grows, and it is possible to have significant dissipation even when  $T < T_c$  and  $I < I_c$ . LA and MH have developed a quantitative theory of thermally activated phase slippage, and this theory provides a good account of a number of experiments.<sup>4-7</sup>

In previous experimental work on this subject the samples were typically  $0.5 \mu\text{m}$  in diameter; this was sufficiently small so as to be one dimensional with regards to superconductivity in the region of interest (i.e., near  $T_c$ ). However, with these samples dissipation could be observed (for low currents) only very near, typically within 1 mK of,  $T_c$ . With modern fabrication techniques it is possible to make structures considerably smaller than those employed in the previous experiments, and this has motivated us to take a new look at this problem. We have fabricated and studied In wires (i.e., very thin and narrow strips) with diameters in the range 400–1000 Å. While the thermal-activation theory is consistent with our results in certain ranges of  $I$  and  $T$ , our findings suggest that there is another process by which phase slippage

can occur. Following a suggestion by Mooij and co-workers,<sup>8</sup> we consider the possibility of quantum tunneling<sup>9,10</sup> *through* the free-energy barrier. While there is at present no quantitative theory of phase slip via quantum tunneling for this system, it is possible to work from analogy with the well-developed theory of macroscopic quantum tunneling (MQT) in other systems to deduce the form that such a theory might take. In this paper we present our experimental results, give a qualitative discussion of the quantum-tunneling process in a one-dimensional superconductor, and compare the predictions of this model with our experiments. As we will see, the experiments appear to be consistent with the quantum-tunneling model.<sup>11-13</sup>

The organization of this paper is as follows. In Sec. II we describe the sample fabrication and the experimental setup. Section III contains a review of the thermal-activation theory and a qualitative discussion of quantum-tunneling effects, both in the low-current limit. Results for the behavior with low measuring currents are given in Sec. IV, and compared with the predictions of Sec. III. The current dependent behavior is considered experimentally and theoretically in Sec. V. Section VI contains a summary, and a discussion of some open questions.

### II. EXPERIMENTAL METHOD

The samples were very narrow In strips (i.e., wires), which were fabricated using a lithographic method described in detail elsewhere.<sup>14,15</sup> First, ion milling is used to produce a vertical step in a substrate; in the present work the substrates were glass. Second, a metal film, in this case In, is deposited so as to cover the step. The film is then milled at an angle so that the metal on the "verti-

cal" edge of the step is in the shadow of the milling beam. The In films were produced by thermal evaporation with the substrates held at 77 K. Cooled substrates were employed to reduce the grain size of the films. In addition, the films were also exposed to a low partial pressure of O<sub>2</sub> while they were warmed to room temperature, as this has been found to reduce agglomeration.<sup>16</sup> The films varied in thickness from 300–1000 Å. Examination with a scanning electron microscope (SEM) indicated a grain size of  $\lesssim 100$  Å. The normal-state resistivity varied systematically with film thickness, and was 4  $\mu\Omega$  cm for the thickest films and 12  $\mu\Omega$  cm for the thinnest ones. The wires had approximately the same residual resistance ratios (i.e., ratio of the room-temperature and low-temperature normal-state resistances) as codeposited films, indicating that they had similar resistivities. The larger resistivity found in the thinnest samples is probably due to the increased importance of boundary scattering. The wires had diameters in the range 400–1000 Å, with the thinnest wires being made from the thinnest films. The sample cross sections were approximately right triangular, and the diameters we quote correspond to  $\sqrt{\sigma}$ , where  $\sigma$  is the cross-sectional area. Selected samples were examined with an SEM, and were found to be very similar in appearance to Au-Pd wires which have been described in great detail in Refs. 14 and 15. The wire diameters appeared to be uniform to within typically 100 Å or better, which was near the resolution limit of the SEM.

The measurements were performed in a <sup>4</sup>He cryostat of standard design, in which the sample was mounted on a thermally isolated copper block which was enclosed in a vacuum can. The cryostat was enclosed in a  $\mu$ -metal shield to reduce the ambient magnetic field, although this was found to not affect the results.

Essentially two different types of measurements were performed. The first was a simple measurement of the resistance as a function of temperature. A battery-powered current supply was employed, and the sample voltage was measured with a digital voltmeter,<sup>17</sup> which was in turn monitored by a microcomputer. Since effects due to outside noise can be a major problem in experiments of this kind, the following precautions were employed. All four sample leads passed through rf filters located at room temperature at the top of the cryostat. Large (10<sup>5</sup>  $\Omega$ ) metal-film resistors located in the vacuum can and at the sample temperature, were placed in series with the samples to provide filtering at low frequencies. In some experiments, room-temperature low-pass filters were also installed, but these were found to have no significant effect. On occasion a low-noise battery operated preamplifier<sup>18</sup> was used to provide additional isolation from the digital voltmeter, and the results were the same as with the arrangement described above. The currents used in these measurements of the resistance as a function of  $T$  were always much less than the critical current, and it was possible to employ currents sufficiently small that the resistance was independent of the measuring current. We also performed several types of measurements as a function of current. These include standard voltage-current measurements, and also measurements (which will be discussed in more detail below) in which

the response of the sample to a time-dependent current was measured. In these cases, the sample current was controlled by the computer, and the voltage was measured using the preamplifier in conjunction with the microcomputer. The same shielding and filtering as described above was employed (but without the room temperature low pass filters).

While great care was taken to isolate the samples from room-temperature noise, this does not guarantee that the effect of this noise was negligible. Possible effects of such noise will be discussed further below.

### III. THEORY: BEHAVIOR AT LOW CURRENTS

#### A. Phase slip by thermal activation

The basis for essentially all of the theoretical discussions in this paper is Ginzburg-Landau (GL) theory. In one dimension the GL free energy can, in situations in which the state of the system is not changing with time, be written in the form<sup>19,2,3</sup>

$$F(\psi) = \frac{\sigma H_c^2 \xi}{4\pi} \int \left[ \left| \frac{\partial \psi}{\partial z} \right|^2 - |\psi|^2 + \frac{1}{2} |\psi|^4 \right] dz, \quad (3.1)$$

where  $H_c$  is the critical field, and  $\xi$  is the coherence length. The GL order parameter can be written as  $\psi = f \exp(i\phi)$ . Near  $T_c$ ,  $H_c$  and  $\xi$  vary as  $H_c = H_{c0}(\Delta T/T_c)^{1/2}$ , and  $\xi = \xi_0(\Delta T/T_c)^{-1}$ , where  $\Delta T \equiv (T_c - T)$ . Note that in (3.1) the distance along the system  $z$  is measured in units of the coherence length, and we have also assumed that the vector potential is zero, which is justified because of the small diameters of the systems we will consider. The stable and metastable states of the system are those for which  $F$  is a local minimum. From (3.1), this implies that  $\psi$  obeys the relation

$$\frac{\partial^2 \psi}{\partial z^2} + (1 - |\psi|^2)\psi = 0. \quad (3.2)$$

If we impose a constant current, (3.2) has a solution

$$\psi = f \exp(ikz), \quad (3.3)$$

where  $f = (1 - \kappa^2)^{1/2}$ , and  $\kappa$  is a parameter which depends on the current density  $J$  through

$$J = \kappa(1 - \kappa^2)cH_c^2\xi/\Phi_0, \quad (3.4)$$

where  $\Phi_0 = hc/2e$  is the flux quantum.

From (3.3) it can be seen that in the presence of a current, this solution for  $\psi$  can be viewed as a helix centered on the  $z$  axis, with the real and imaginary parts of  $\psi$  being the transverse "directions" of the helix.<sup>1,2</sup> This helix becomes wound more tightly as  $J$  is increased. Following LA and MH we impose periodic boundary conditions on  $\psi$ , which restrict  $\kappa$  to discrete values  $2\pi n/L$ , where  $n$  is an integer, and  $L$  is the length of the system. Hence  $n$  is the number of loops in the helix. From (3.3) and (3.1) one can show that the GL free energies of these states are

$$F = -\frac{\sigma \xi L H_c^2}{4\pi} \frac{(1 - \kappa^2)^2}{2}. \quad (3.5)$$

LA showed that for each of the states (3.3) the free energy is a local minimum in  $\psi$  space, and thus if one is to pass continuously from one of these minima to an adjacent one, it is necessary to pass over a free-energy barrier. This process corresponds to addition or removal of a single phase loop from the  $\psi$  helix, and is referred to as phase slip, since it changes the phase of  $\psi$ . Little<sup>1</sup> estimated the height of this barrier qualitatively from the following argument. If one assumes that  $\psi$  must vary continuously, the only way one can change the value of  $n$ , i.e., add or remove a phase loop, is to have the magnitude of  $\psi$  go to zero. Little argued that this would occur in a localized region of space, and since  $\psi$  cannot vary appreciably over distances less than  $\xi$ , the lowest energy fluctuation of this type is one in which  $|\psi|$  vanishes, i.e., the system becomes “normal,” over a length of order  $\xi$ . Since the condensation-energy density is of order  $H_c^2$ , and  $\xi\sigma$  is the volume of the fluctuation region, the energy cost for such a fluctuation to the normal state is  $H_c^2\xi\sigma$ . LA considered this process in more detail, and found that in the limit  $J \rightarrow 0$  the free-energy barrier is given by

$$\Delta F_0 = \sqrt{2}H_c^2\xi\sigma/3\pi, \quad (3.6)$$

which apart from a numerical factor is the same as Little’s result.

It is also important to consider the effect of  $J$  on the free-energy barrier. In the presence of a dc current there is a  $J$ -dependent shift of the free energies of the current-carrying states, (3.5). This causes a “tilt” in the free-energy diagram, resulting in the well-known washboard potential,<sup>20</sup> shown in Fig. 1. The free-energy difference between two adjacent minima in  $F$ , i.e., minima that describe states  $\psi$  which are separated by  $\Delta n = \pm 1$ , is given by

$$\Delta F_I = \pm \Phi_0 \sigma J / c. \quad (3.7)$$

The free-energy barrier that must be surmounted for a variation of  $\psi$  which reduces the current is  $\Delta F_0 - \Delta F_I/2$ , while for a variation that increases  $J$  one has a barrier  $\Delta F_0 + \Delta F_I/2$ .

With this picture of the free-energy landscape in mind, the thermal activation model of phase slippage can be expressed as follows. For a constant current, the system is described by a helix with a certain number of phase loops. Continuous variations of  $\psi$  that add or remove a

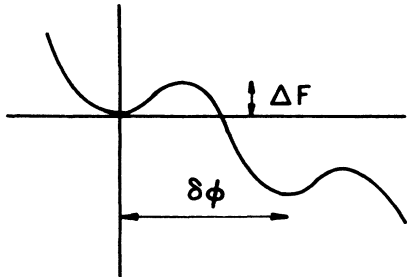


FIG. 1. Schematic of the “washboard” potential. The barrier height  $\Delta F$  and the distance under the barrier  $\delta\phi$  are indicated.

loop involve passing over the free-energy barriers already described. From the Josephson relation, these variations yield a voltage

$$\Delta V = \frac{\hbar}{2e} \frac{\partial \Delta\phi}{\partial t}, \quad (3.8)$$

where  $\Delta\phi$  is the phase difference across the system and  $\Delta V$  is the voltage difference. If the system starts in one of the minima of Fig. 1, then one would expect that thermal activation will result in transitions out of this state at a rate

$$\Gamma_{TA} = \Omega \exp[-(\Delta F_0 \pm \Delta F_I/2)/k_B T], \quad (3.9)$$

where  $\Omega$  is an attempt frequency, and the  $\pm$  signs correspond to transitions that increase and decrease the current, respectively. These transition rates can be converted into a voltage across the system, and hence to an effective resistance,<sup>2</sup> using (3.8), since each transition changes  $\phi$  by an amount  $2\pi$ .

It remains to estimate the attempt frequency  $\Omega$  in (3.9). The discussion to this point has involved only static properties, and hence the time-independent GL equation has been sufficient. However, a calculation of the attempt frequency requires some knowledge of the dynamics. This problem has been considered by MH, who employed the time-dependent GL equation, which can be written in the form<sup>3,19</sup>

$$\frac{\partial \psi}{\partial t} = -\frac{4\pi}{\sigma H_c^2 \xi \tau} \frac{\delta F}{\delta \psi^*}, \quad (3.10)$$

where we again assume that the vector potential is zero. Equation (3.10) describes the time-dependent behavior for small changes of  $F$  near a minimum. This behavior is seen to be purely diffusive, with a relaxation time<sup>19</sup>

$$\tau = \frac{\pi \hbar}{8k_B(T_c - T)}. \quad (3.11)$$

While the time independent GL equation has a firm theoretical foundation and is widely applicable, the time-dependent theory has, as noted by MH and by many other workers, a number of limitations.<sup>19</sup> It is not at all clear that this equation describes, even qualitatively, the dynamics below  $T_c$  of a superconductor with a nonzero energy gap such as In. Nevertheless, we will employ (3.10) in nearly all of our discussions, although we will also point out places where limitations of (3.10) appear to be most serious.

Using (3.10), MH calculated the attempt frequency  $\Omega$  which enters the thermal-activation rate. In the limit of low current they find

$$\Omega = \left[ \frac{\sqrt{3}L}{2\pi^{3/2}\xi\tau} \right] \left[ \frac{\Delta F_0}{k_B T} \right]^{1/2}. \quad (3.12)$$

As discussed by MH, this result has a fairly simple interpretation.  $\tau$  is the only time scale in the problem, so it is natural that  $\Omega \sim \tau^{-1}$ . A phase slip can occur anywhere along the system, and since it involves a length of order  $\xi$ , there are roughly  $L/\xi$  different places where a phase slip can occur, hence one expects  $\Omega \sim L/(\xi\tau^{-1})$ , as found in

(3.12). The last factor in (3.12) is not as obvious,<sup>3</sup> but is typically of order unity, so it does not have a large affect on the magnitude of  $\Omega$ .

Combining (3.9) and (3.12), the resistance below  $T_c$  can, in the low-current limit, be written as<sup>2,3,21</sup>

$$R_{TA} = \frac{\Phi_0 \Omega}{I_1} \exp(-\Delta F_0 / k_B T), \quad (3.13)$$

where  $I_1 = k_B T / \Phi_0$ . Near  $T_c$ ,  $\Delta F_0$  goes to zero as  $(\Delta T)^{3/2}$ , and since this factor enters in the exponent in (3.13), it dominates the temperature dependence of  $R_{TA}$ . It is important to note that the result (3.9) and hence (3.13) is only applicable when  $\Delta F_0 \gg k_B T$ , due to limitations involved in deriving the basic thermal-activation result (3.9).<sup>22</sup> Since  $\Delta F_0$  vanishes at  $T_c$ , this means that (3.13) will not apply very near  $T_c$ . We should also emphasize that these results for the thermal-activation rate (3.9) and the associated resistance (3.13) apply only for small currents. The case of currents that are not small will be considered in Sec. V.

The prediction (3.13) of the thermal activation model has been tested in several experiments.<sup>4-7</sup> Most of these experiments have involved samples with diameters in the neighborhood of 5000 Å, and the results are generally in good agreement with the thermal activation theory.<sup>7</sup>

### B. Phase slip by quantum tunneling

As we will see in Sec. IV, our results indicate that the thermal activation model does not provide a complete picture of the observed behavior, and that some other mechanism for phase slippage dominates at temperatures more than a few tenths of a degree below  $T_c$ . Mooij and co-workers<sup>8</sup> have suggested that phase slippage could occur via quantum tunneling. This process would be analogous to the macroscopic quantum tunneling (MQT), which has been studied a great deal in recent years in connection with tunnel junctions, superconducting quantum-interference devices, and other systems. We will therefore refer to this mechanism for phase slippage in our system as MQT. To the best of our knowledge, the only theoretical treatment of MQT in a one-dimensional superconductor is that of Saito and Murayama.<sup>23</sup> However, that theory considers only the behavior for  $T \approx 0$ , and is therefore not applicable to our experiments. While there is no detailed theory of phase slip by MQT in a one-dimensional superconductor in the regime relevant for our work, one can to some extent work from analogy with the situation in tunnel junctions to construct semi-quantitative predictions for this case.

The behavior of a tunnel junction is analogous<sup>9,10,24,25</sup> to the motion of a damped particle moving in a potential like that shown in Fig. 1. In this case the equation of motion is

$$m\ddot{q} + \eta\dot{q} + \frac{\partial V}{\partial q} = F_{\text{ext}}, \quad (3.14)$$

where  $q$  is the spatial coordinate of the particle,  $m$  is its mass,  $V$  is the potential energy,  $F_{\text{ext}}$  is the force acting on the particle, and  $\eta$  is a damping parameter that arises

from the interaction of the particle with its environment. The behavior of a particle described by (3.14) has attracted a great deal of theoretical attention recently, and the rate for tunneling from one metastable minimum to an adjacent one has been shown to in general be a complicated function of the damping, temperature, etc.<sup>25,26</sup> For simplicity we will consider only the lowest-order results for the tunneling rate in two limits, underdamped and overdamped. In both cases, the tunneling rate can be written in the form<sup>9,10,26,27</sup>

$$\Gamma_{\text{MQT}} = A e^{-B}, \quad (3.15)$$

where  $A$  and  $B$  are parameters that we now discuss. It has been shown that in the limit of weak damping<sup>9,10</sup>

$$A = 12 \left[ \frac{3}{2\pi} \right]^{1/2} \left[ \frac{V_0 \omega_0}{\hbar} \right]^{1/2}, \quad B = \frac{7.2 V_0}{\hbar \omega_0}, \quad (3.16)$$

where  $V_0$  is the barrier height, and  $\omega_0$  is the frequency for small oscillations of the particle about the free-energy minimum. If the damping is strong, one has instead<sup>28,29</sup>

$$A = 8\sqrt{6} \omega_0 \alpha^{7/2} \left[ \frac{V_0}{\hbar \omega_0} \right]^{1/2}, \quad B = \frac{2\pi \eta (\delta q)^2}{9\hbar}, \quad (3.17)$$

where  $\eta$  is the viscosity [see (3.14)],  $\alpha = \eta / 2m\omega_0$ , and  $\delta q$  is the distance that the particle must tunnel under the barrier.

Let us now return to our equation of motion, the time dependent GL equation (3.10), in order to identify quantities such as  $\eta$ , etc. One immediately sees that it is not possible to make a strict analogy between our problem and that of a particle moving in a potential according to (3.14). The difficulty is that the equation of motion (3.10) is purely diffusive, and thus has no mass term. Hence, it is not possible to use (3.10) to determine quantities analogous to  $m$  and  $\omega_0$ , which play a key role in the predictions for the tunneling rate, (3.16) and (3.17). We must therefore proceed phenomenologically, but before we do, it is important to note that the shortcomings of (3.10) with respect to this problem do not necessarily imply any fundamental difficulty with the analogy. That is, there may still exist a close analogy between a one-dimensional superconductor and a particle moving in a washboard potential. There have in recent years been a number of theoretical treatments of the dynamical, i.e., nonequilibrium, properties of superconductors, and the existence of a variety of propagating modes has been amply demonstrated,<sup>30,31</sup> both theoretically and experimentally. This suggests that an equation of motion with a mass term, as in (3.14), could well be appropriate for our problem. Hopefully this question will attract theoretical attention in the near future.

Returning to the problem of making a qualitative estimate of  $A$  and  $B$ , we first consider the underdamped case. It is clear that we must identify  $\Delta F_0$  with  $V_0$ , the problem is how to choose  $\omega_0$ . Since  $\tau$  is the only time scale in time-dependent GL theory, a natural choice is to identify  $\tau^{-1}$  with  $\omega_0$ . We emphasize that there is no fundamental justification for this choice [although a similar result was found for  $\Omega$  in (3.12)]; theoretical guidance here would be

most welcome. In any case, with these choices for  $V_0$  and  $\omega_0$  one finds

$$A = 12 \left[ \frac{3}{2\pi} \right]^{1/2} \left[ \frac{\Delta F_0}{\hbar\tau} \right]^{1/2}, \quad B = \frac{7.2\Delta F_0\tau}{\hbar}. \quad (3.18)$$

Let us next consider the situation for strong damping. Here we again identify  $\Delta F_0$  with  $V_0$ , and  $\tau^{-1}$  with  $\omega_0$ . We must now also deal with  $\delta q$ ,  $\eta$ , and  $m$ . The distance under the barrier is, from (3.10), analogous with  $\delta\phi$ , since this is the "distance" that our system tunnels. The distance between metastable minima in Fig. 1 is  $\Delta\phi \sim 2\pi$ , so we estimate  $\delta\phi \sim 1$ . Comparing the time dependent GL equation with (3.14), we see that  $\sigma H_c^2 \xi \tau / 4\pi$  plays the role of  $\eta$ , so we have  $\eta = 3\Delta F_0 \tau / 4\sqrt{2}$ . Estimating  $m$  is again a problem. However, given that we have already identified  $\tau^{-1}$  with  $\omega_0$ , we can use the fact that the frequency for small oscillations in Fig. 1 can be written as

$$\omega_0 = \left[ \frac{1}{m} \frac{\partial^2 V}{\partial q^2} \right]^{1/2}. \quad (3.19)$$

When the washboard is tilted such that the barrier in Fig. 1 is small, the potential is well approximated by a cubic form,<sup>10</sup>

$$V \approx \frac{27}{4} V_0 \left[ \left( \frac{q}{q_0} \right)^2 - \left( \frac{q}{q_0} \right)^3 \right], \quad (3.20)$$

where we have assumed that there is a minimum at  $q=0$ , and that the distance under the barrier is  $q_0$ . Assuming  $q_0=1$ , as above, this leads to  $\partial^2 V / \partial q^2 = 27V_0/2$ . Using this with (3.19) we find

$$m = \frac{27V_0}{2\omega_0^2} = \frac{27\Delta F_0\tau^2}{2}, \quad (3.21)$$

where we have also used our earlier results for  $V_0$  and  $\omega_0$ . From (3.21) we find  $\alpha = 1/36\sqrt{2}$ , independent of temperature, and this leads to

$$A = \frac{8\sqrt{2}}{(36\sqrt{2})^{7/2}} \left[ \frac{\Delta F_0}{\hbar\tau} \right]^{1/2}, \quad B = \frac{\pi}{6\sqrt{2}} \frac{\Delta F_0\tau}{\hbar}. \quad (3.22)$$

In our earlier work,<sup>12</sup> we derived  $A$  and  $B$  in the overdamped limit with the assumption that  $\alpha$  was a constant. We see now that this assumption is equivalent to the identification of  $\tau^{-1}$  with  $\omega_0$ . Hence, the approach used here is equivalent to the one used in our previous analysis.

It is interesting to compare the results for the tunneling rate in the underdamped and overdamped limits. We see from (3.18) and (3.22) that aside from some numerical factors, the parameter  $A$  is the same in the two cases. Most importantly, the temperature dependence of  $A$  is precisely the same in the two limits. In addition, apart from a numerical factor of order unity,  $B$  is the same in the two limits. That this would turn out to be the case was not at all obvious from our initial assumptions. It also leads one to hope that the conclusions drawn from the analysis below may be largely independent of any assumptions concerning the strength of the damping.

Putting all of these results together, our arguments suggest that quantum tunneling should proceed at a rate

$$\Gamma_{\text{MQT}} = \beta_1 \frac{L}{\xi} \left[ \frac{\Delta F_0}{\hbar\tau} \right]^{1/2} \exp \left[ -\beta_2 \frac{\Delta F_0\tau}{\hbar} \right], \quad (3.23)$$

where the factor  $L/\xi$  has been inserted since it is the number of independent locations along the system at which a phase-slip event can occur [the same factor is present in (3.12)]. The factors  $\beta_1$  and  $\beta_2$  in (3.23) are constants that can be obtained from either (3.16) or (3.22), depending on whether the system is underdamped or overdamped. In analogy with the case for thermal activation, (3.23) leads to an effective resistance at low currents which is given by<sup>32</sup>

$$R_{\text{MQT}} = \frac{\Phi_0^2 \beta_1 \beta_2 \tau}{\hbar} \frac{L}{\xi} \left[ \frac{\Delta F_0}{\hbar\tau} \right]^{1/2} \exp \left[ -\beta_2 \frac{\Delta F_0\tau}{\hbar} \right]. \quad (3.24)$$

In general, we would expect that both thermal activation and quantum tunneling could take place. Assuming that they occur in parallel, the total resistance would then be the sum of (3.13) and (3.24).

#### IV. TEMPERATURE DEPENDENCE OF THE RESISTANCE

##### A. Results

As discussed in Sec. II, the samples were fabricated from thin films; a few films from each evaporation batch were always kept aside so that their properties could be compared with those of the wires. A noteworthy property of the films was that their critical temperatures were all well above the standard value for bulk In, which is  $\approx 3.4$  K. This can be seen from Fig. 2, which shows typical results for a 410 Å wire, and a codeposited film which was approximately 300 Å thick. Previous workers have also reported critical temperatures for In films that were well above bulk values.<sup>33</sup> As in our experiments, that work involved In films evaporated onto cooled substrates.

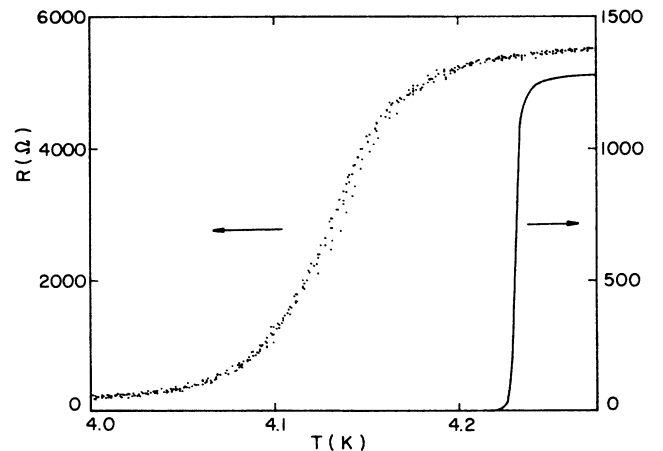


FIG. 2. Resistance as a function of temperature for a 410 Å wire (points, left hand scale) and a co-deposited film (solid line, right hand scale). Note that the transition is much sharper in the film.

The increase of  $T_c$  in the films has been attributed to changes in the electron-phonon coupling.<sup>33</sup> Whatever the cause, this behavior does not appear to be important for the present discussion.<sup>34</sup> We also note from Fig. 2 that the transition width of the film is much smaller than that of the wire, indicating that the effects of inhomogeneities in the films are negligible on the scale of interest to us here.

Figure 3 shows some typical results for the resistance as a function of temperature for two wire samples. To within the experimental uncertainties, these results are independent of measuring current, for the currents employed (typically  $\lesssim 10^{-8}$  A).<sup>35</sup> The larger wire is seen to have a somewhat narrower transition, and its resistance vanishes more rapidly below  $T_c$  than does that of the smaller wire, whose resistance approaches zero very slowly as the temperature is reduced. It is useful to consider this behavior on logarithmic scales, as shown in Fig. 4. Here it is seen that the low-temperature behavior of the two samples is indeed quite different. In particular, the behavior of the small sample exhibits an abrupt crossover at  $T_c - T \approx 0.2$  K. Such a crossover is not seen for the larger wire, although we will argue below that this behavior would be seen if the measurements could be extended to lower temperatures. Unfortunately, the resistance of the larger wire at  $T_c - T \lesssim 0.2$  K is below our sensitivity. We will see later how one can probe the low temperature region with a different type of measurement.

Returning to Fig. 4, let us now compare these results with the theory discussed in the preceding section. Considering first the 745 Å sample, the solid line in Fig. 4 is the prediction of thermal activation theory (3.13), and was obtained as follows. The theory depends sensitively on a number of parameters, hence one approach would be to simply perform a least-squares fit to the experimental data. However, performing such a fit is complicated by the fact that the theory is expected to break down when the transition rate becomes large, i.e., near  $T_c$ , and it is difficult to know precisely how close to  $T_c$  one should expect the theory to be accurate. This and other complica-

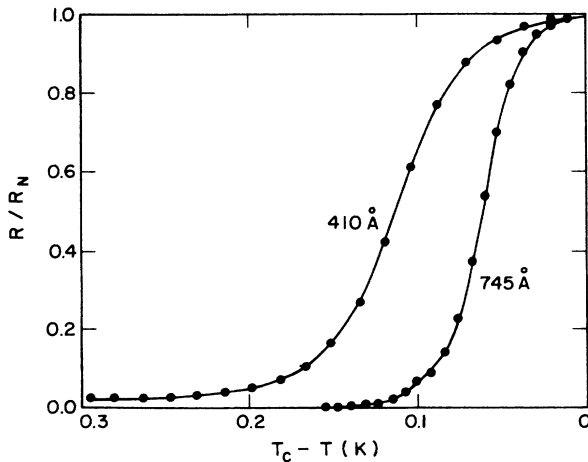


FIG. 3. Resistance, normalized by the normal state value, as a function of temperature for a 410 Å wire and a 745 Å wire. The smooth curves are simply guides to the eye.

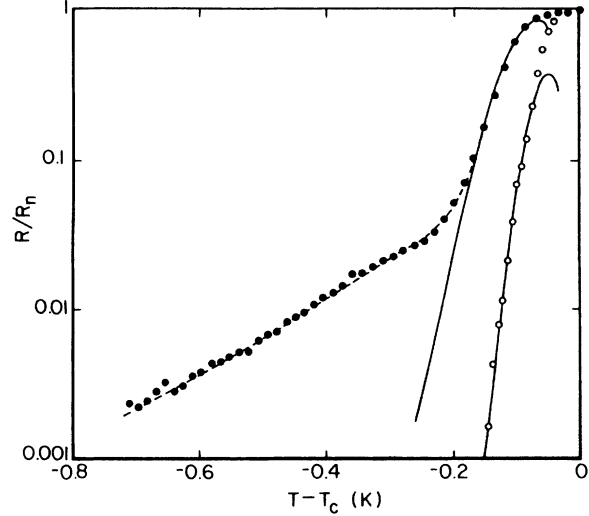


FIG. 4. Same data as in Fig. 3, but with a logarithmic vertical axis. The lines are the theory, and are discussed in the text.

tions were encountered in previous comparisons of the thermal activation theory with data on much larger samples.<sup>4-7</sup> In those comparisons it was found that the quality of such a fit was relatively insensitive to rather large variations of the prefactor  $\Omega$ , (3.12), and great care was necessary in order to make meaningful comparisons with the theory. In view of all this, and also the fact that our expression for the quantum-tunneling rate is at best only qualitative, we will in the following emphasize the qualitative features of the data, and attempt to draw conclusions which are as model independent as possible. We have therefore not performed detailed least squares fits, but rather have chosen to hold many of the relevant parameters fixed, using estimates based on independent experiments or theory, and have incorporated only a few adjustable parameters which we now discuss.

In comparing the data in Fig. 4 with thermal activation theory (3.13) there are two key parameters,  $\Omega$  and  $\Delta F_0$ . These in turn depend on  $H_c$ ,  $\xi$ ,  $\sigma$ ,  $L$ , and  $\tau$ . The cross-sectional area  $\sigma$  and length  $L$  can be accurately estimated,<sup>15</sup> and so are not a problem. We use the standard expressions<sup>36</sup> for  $H_c$  and  $\xi$  [see the discussion in connection with (3.1)], with the previously measured values<sup>37</sup> of  $H_c(T=0)$  and  $\xi(T=0)$ , take  $\tau$  from (3.11), and obtain  $T_c$  from the measurements on codeposited films (Fig. 2). To allow for uncertainties in these values and in the theory, we employ two adjustable factors associated with  $\Omega$  and  $\Delta F_0$ , respectively. In evaluating the theory (3.13) we multiply  $\Omega$  from (3.12) by a factor  $\gamma_1$ , and  $\Delta F_0$  from (3.6) by a factor  $\gamma_2$ , so that the prediction then reads

$$R_{TA} = \gamma_1 \frac{\Phi_0 \Omega}{I_1} \exp(-\gamma_2 \Delta F_0 / k_B T). \quad (4.1)$$

$R_{TA}$  is most sensitive to the value of the exponent, and this value largely determines the slope seen in Fig. 4. Changes in the prefactor in (4.1) (i.e., in  $\gamma_1$ ) shift the curve in Fig. 4 vertically, but do not change its shape. The theoretical curve for the large wire in Fig. 4 was ob-

tained with  $\gamma_1=0.01$ , and  $\gamma_2=0.05$ . These values are discussed in detail in the Appendix. Here we note that this result for  $\gamma_2$  suggests that the values employed for quantities such as  $H_{c0}$  or  $\xi_0$ , may be incorrect. This would not be surprising, given that  $T_c$  is different from the bulk value. There is also the possibility that the values of  $\gamma_1$  and  $\gamma_2$  are affected by the presence of external noise, and this will be discussed in Sec. V A. Yet another possibility is that our choice of  $T_c$  is not correct.<sup>38</sup> In fact, a small downward shift of  $T_c$  would increase the value of  $\gamma_2$ , by a factor of 2 or more. In any case, the values of  $\gamma_1$  and  $\gamma_2$  we find are not out of line with the values of similar parameters which were found in previous comparisons with thermal activation theory. One also sees from Fig. 4 that the thermal activation theory breaks down dramatically near  $T_c$ . As noted above, this is expected, and has been observed in previous work. Changing  $\gamma_1$ ,  $\gamma_2$ , etc., does not appreciably affect the manner in which the theory fails near  $T_c$ . In spite of all of these potential complications, we believe that the important point to note from Fig. 4 is that the results for the large sample are consistent with the form predicted by the thermal activation theory.

Figure 4 also shows a comparison with thermal activation theory for the 410 Å sample. We see that thermal activation theory is consistent with the form found near  $T_c$  (although we again see a breakdown of the theory very near  $T_c$ ). The values of  $\gamma_1$  and  $\gamma_2$  used in evaluating thermal activation theory for the small sample were 1 and 0.3, respectively, so the quantitative agreement with (3.13) is again satisfactory (and in fact better than for the larger wire, since  $\gamma_1$  and  $\gamma_2$  are closer to unity). Returning to Fig. 4, we see that for the small sample when  $T_c - T \approx 0.2$  K the results deviate *qualitatively* from the prediction of thermal activation theory. We emphasize that the thermal activation expression (3.13) is *not* capable of exhibiting the change in slope seen at  $T_c - T \approx 0.2$  K in Fig. 4. These results therefore indicate that there is some other mechanism for phase slippage in this region, and we now consider if the quantum-tunneling prediction (3.24) can explain this behavior. The dashed line in Fig. 4 shows the prediction of a sum of the resistances (which is simply proportional to a sum of the phase-slip rates) due to thermal activation and quantum tunneling. The idea here is that thermal activation dominates near  $T_c$ , while quantum tunneling is important at lower temperatures. In comparing with the quantum-tunneling expression (3.24), we have treated the parameters  $\beta_1$  and  $\beta_2$  as adjustable. The values of these parameters needed to obtain the dashed curve in Fig. 4 are given in Table I, and will be discussed below.<sup>39</sup> The point we wish to emphasize here is that the overall *qualitative* behavior seen for the small sample in Fig. 4 is in good agreement with the *form* predicted by a theory which includes both quantum tunneling and thermal activation. The crossover seen at  $T_c - T \approx 0.2$  K is thus due to a change in the dominant phase-slip mechanism; thermal activation at higher temperatures and quantum tunneling at lower temperatures.

The behavior found in Fig. 4 has been observed in a number of different samples. Results for several addition-

al samples are given in Fig. 5, and Table I lists the corresponding values of the parameters  $\gamma_1$ ,  $\gamma_2$ ,  $\beta_1$ , and  $\beta_2$ , which were found to yield good agreement with the theory (e.g., the solid curves in Fig. 5). It is seen from Table I that the barrier-height parameter  $\gamma_2$  seems to become smaller as the wire diameter is increased. The reason for this trend is not completely clear, but it could easily be due to small systematic errors in our choice of parameters<sup>38</sup> such as  $T_c$ .

Let us now consider the crossover from thermal activation to quantum tunneling. Comparing the thermal and quantum-tunneling transition rates, (3.9) and (3.23), we see that the former is proportional to  $\exp(-\gamma_2 \Delta F_0 / k_B T)$ , while the latter is proportional to<sup>39</sup>  $\exp(-\gamma_2 \beta_2 \Delta F_0 / \hbar \tau^{-1})$ . The prefactors are also similar (though not identical), but since the exponential factors dominate, we will only consider them here. With this approximation the transition rates are equal when  $k_B T$  is of order  $\hbar \tau^{-1}$ . Using (3.11) this condition can be written as

$$T_c - T \approx \frac{\pi \beta_2 T}{8}. \quad (4.2)$$

Hence we would expect to observe a crossover from thermal activation near  $T_c$  to quantum tunneling far from  $T_c$ , at a temperature given by (4.2), and this is indeed seen in Figs. 4 and 5. In addition, (4.2) shows that the crossover from thermal activation to quantum tunneling should occur at a temperature which is *independent* of the size of the sample. Hence, we would expect to find this crossover in *all* samples, including the large one in Fig. 4, and also the much larger samples studied in previous work.<sup>4-6</sup> The reason this crossover is not seen in the large wire in Fig. 4 is that the resistance at the crossover temperature is extremely small, well below our sensitivity. Thus while we expect that quantum tunneling should also take place in very large samples, a simple resistance measurement is not always the easiest way to observe it. We will return to this point below.

This consideration of the exponential factors that dominate the transition rates also shows clearly why the rates of thermal activation and quantum tunneling have different temperature dependences. The temperature dependence of the thermal rate is essentially just  $\exp(-\Delta F_0 / k_B T)$ , while that of the quantum tunneling rate is  $\exp(-\Delta F_0 / \hbar \tau^{-1})$ . Since  $\Delta F_0 \sim (\Delta T)^{3/2}$  and  $\tau \sim (\Delta T)^{-1}$ , it is clear that quantum tunneling will have a *weaker* temperature dependence than thermal activation. This is the reason for the crossover seen in Figs. 4 and 5.

## B. Potential experimental problems

We have shown that the results of our resistance measurements are consistent with the mechanism of quantum tunneling already outlined. At this point it is worthwhile to consider several potential experimental complications, which one might imagine could lead to similar results.

First, one must consider the effects of external noise. Even though great care was taken in filtering the sample leads, it is very difficult to know if one has really eliminated all effects of outside noise. This is an especially

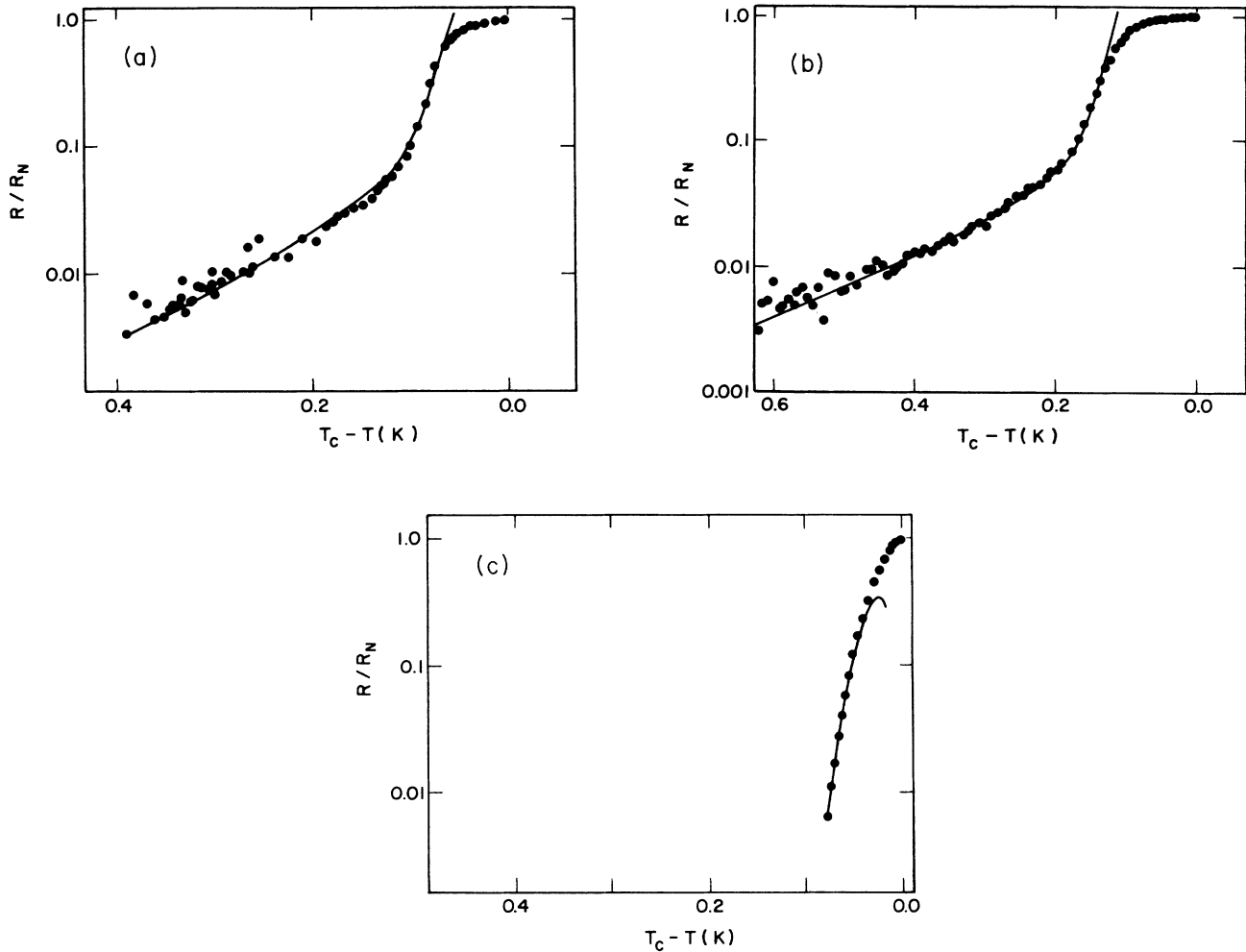


FIG. 5. Resistance, normalized by the normal state value, as a function of temperature for several samples. (a) 420 Å sample; (b) 485 Å sample; (c) 1010 Å sample. The lines are the theory, taking into account both thermal activation and quantum tunneling, as discussed in the text.

severe problem in experimental studies of thermal activation and macroscopic quantum tunneling in tunnel junctions and similar systems.<sup>40–47</sup> However, one would not expect external noise to influence the qualitative behavior seen in Figs. 4 and 5 for the following reason. The energy barrier  $\Delta F_0$  becomes larger as  $T_c - T$  increases. The external noise level (if indeed any is present) should be roughly independent of temperature (over the relatively narrow range of interest to us here), hence the effects of such noise should be largest near  $T_c$ . This is the regime where thermal activation dominates, and the thermal activation form describes the experiments fairly well, suggesting that external noise is not a major problem. At low temperatures where quantum tunneling is important, the energy barrier is much larger, and thus the relative size (and effect) of any external noise would be much smaller. It therefore appears that spurious noise is *not* responsible for the low temperature behavior, which we have attributed to quantum tunneling. Note that arguments of this kind cannot be used in analyzing the effect of noise on tunnel junctions, since in that case the barrier

height is constant (in the range of interest), and quantum tunneling becomes important only at very low *absolute* temperatures. The effects of external noise will be discussed further in Sec. V A.

Another concern is sample homogeneity. As we have noted in Sec. II, electron microscopy indicates that the degree of homogeneity is similar to that of Au-Pd wires made with the same technique, which have been employed extensively in studies of localization and electron-electron interactions.<sup>15,48</sup> Sample inhomogeneity does not appear to have been a problem in those experiments. Nevertheless, it is worth considering what effect inhomogeneities in the cross-sectional area would have in the present work. There will always be places along a sample at which the cross-sectional area is smaller than the average value. The energy barrier  $\Delta F_0$  will be smaller at these locations, since it is proportional to  $\sigma$ . The rate of phase slippage, due to either thermal activation or quantum tunneling, depends exponentially on  $\Delta F_0$ , so the phase slips will occur preferentially at these locations. Such behavior is unavoidable, but it will not affect the



qualitative form of the resistance. Assuming that the inhomogeneity is not too large, the barrier height will be approximately the same as that calculated from (3.6) using the average cross-sectional area. However, the attempt frequency (3.12) and also the prefactor for the quantum tunneling rate (3.23) will in this case not be proportional to the length of the sample, but rather will scale as the number of sites at which phase slippage occurs. Hence, the factors of  $L/\xi$  in (3.13) and (3.24) will be replaced by temperature independent constants of order unity. Since the temperature dependences of the transition rates are dominated by the exponential factors, this change will have very little effect on the theoretical curves in Figs. 4 and 5, although it will lead to values of  $\gamma_1$  and  $\beta_1$  that are less than unity.

From this discussion we conclude that these potential experimental complications are not capable of accounting for the behavior we have attributed to quantum tunneling.

## V. BEHAVIOR AS A FUNCTION OF CURRENT

### A. Overall behavior

Figure 6 shows some results for the voltage  $V$  as a function of current for a 720 Å wire. In these measurements the current was increased continuously starting from zero, and the sample is seen to switch abruptly into the finite-voltage state.<sup>49</sup> It has been shown<sup>40,41</sup> that measurements of the current at which this switching occurs can be used to determine the transition rate of the system out of the free-energy minima in Fig. 1. The basic idea can be understood by considering again the washboard potential (Fig. 1). An applied current acts to tilt the washboard, and hence reduces the energy barrier for transitions to states corresponding to smaller currents. If the current is gradually increased, the system becomes absolutely unstable to phase slip at the critical current,  $I_c$ ; at this point the minima in Fig. 1 become inflections in the free-energy curve. However, for currents just

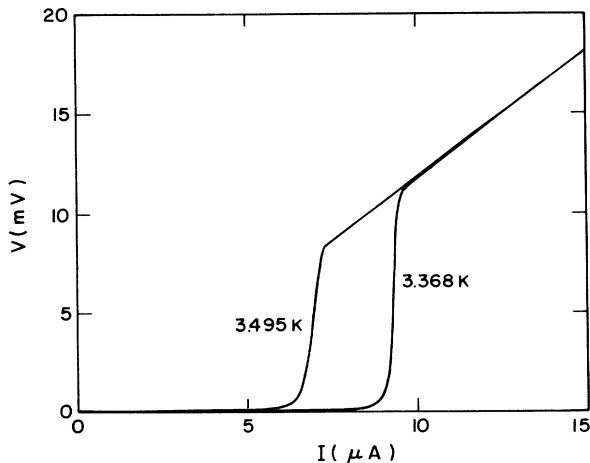


FIG. 6.  $V$ - $I$  measurement for a 720 Å wire.

below  $I_c$ , the energy barrier is very small, and before one reaches  $I_c$  it is possible for a thermal fluctuation, or a quantum-tunneling event, to carry the system over, or through, the reduced energy barrier. Hence this first phase-slip event will occur before  $I_c$  is reached. If the system is sufficiently underdamped, it will maintain enough "kinetic" energy to pass over succeeding barriers. It will thus move continuously down the washboard, which corresponds to being in the finite voltage state. A thermal fluctuation, or quantum tunneling, event will be a stochastic process, so the value of  $I$  at which the first phase slip occurs will be distributed over some range. By measuring this probability distribution,  $P(I)$ , one can use the known dependence of the potential on  $I$  to obtain the transition rate as a function of  $I$ .

The discussion in Sec. III was concerned only with the case  $I \rightarrow 0$ ; the results quoted there do not yield any information concerning quantities such as the energy barrier and attempt frequency for currents near  $I_c$ . This case was considered by LA and MH, and their results will be discussed below. However, we will first consider the experimental results for  $P(I)$ .

Measurements of the distribution  $P(I)$  are straightforward, and were performed as follows.<sup>40,41</sup> Starting from zero, the current was increased at a constant rate, and the sample voltage was monitored continuously. When  $V$  exceeded a certain trigger level (typically 1 mV), the value of  $I$  was recorded. The current was then reset to zero, and the process repeated many times. In previous measurements of this kind for tunnel junctions,<sup>41-47</sup> typically  $10^4$  or more switching events were recorded, a process taking anywhere from a few minutes to the order of an hour or more. However, in our experiments it was found that there was a small but non-negligible amount of Joule heating when the sample switched into the finite voltage state, and it was necessary to wait for a period of time

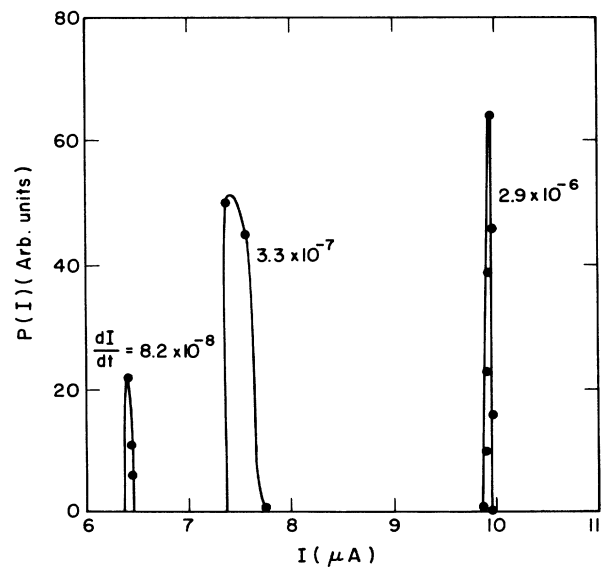


FIG. 7. Distribution of  $I_s$  as a function of  $I$  for a 720 Å sample at  $T=3.502$  K ( $T_c=3.733$  K for this sample), for three different sweep rates as given in the figure. The lines are guides to the eye.

after resetting the current to zero to permit the sample temperature to return to its initial value. The time delay required was typically 30–60 s. This greatly limited the number of switching events which could be collected, with typical numbers being a few hundred. While high-resolution measurements of  $P(I)$  could thus not be made in this way (without excessively long measuring times), it was nevertheless possible to obtain semi-quantitative results, and some results for  $P(I)$  are shown in Fig. 7. Here we show results for a fixed temperature, and for several different current sweep rates. For each sweep rate the distribution is seen to be fairly narrow, although the width is somewhat larger than the available resolution limit set by the sensitivity of the electronics, temperature drift, etc.

We could in principle use these results for  $P(I)$  to ex-

tract<sup>41</sup> the transition rate  $\Gamma(I)$ . However, because we have been able to sample only a relatively small number of switching events, we have chosen to take a different approach. The transition rate will in general be very small for small  $I$ , and increase rapidly at a value  $I=I_s$ , as can be seen from the results for  $P(I)$  in Fig. 7. Let  $\delta I_c$  be the width of the switching distribution, and  $dI/dt$  be the rate at which the current is varied. Switching will occur when  $\Gamma\delta I_c/(dI/dt)\sim 1$ , since  $\delta I_c/(dI/dt)$  is the time spent sweeping through the distribution.<sup>50</sup> Thus, the quantity  $dI/dt$  will be proportional to  $\Gamma$  at  $I_s$ . In the measurements, the current, which was initially zero, was increased at a rate of typically a few  $\mu\text{A/s}$ , and  $I_s$ , the value of  $I$  at which  $V$  exceeded a given trigger level, was recorded. The sweep speed was then varied, and  $I_s$  was measured as a function of  $dI/dt$ . Figure 8 shows results

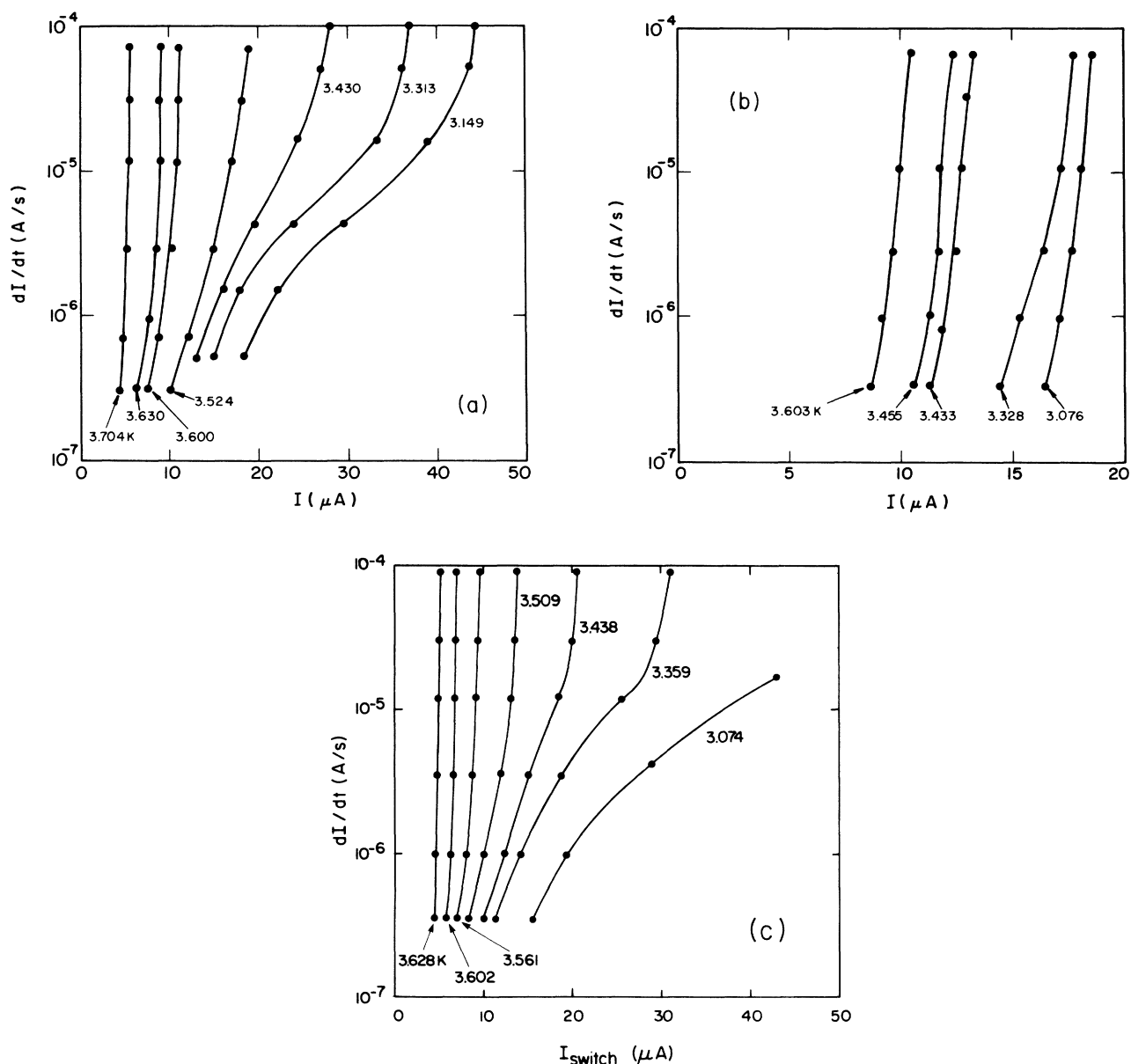


FIG. 8. Speed at which the current is swept as a function of the current,  $I_s$ , where the sample switches into the finite voltage state, at several temperatures. (a) 640 Å sample; (b) 520 Å sample; (c) 1010 Å sample. The lines are guides to the eye.

for  $dI/dt \sim \Gamma$  as a function of  $I_s$ , at several temperatures, for three different samples. Figures 8(a) and (c) correspond to fairly large samples that did not exhibit quantum tunneling in measurements of the resistance as a function of temperature (Figs. 4 and 5), while Fig. 8(b) is a fairly small sample that did display the signature of quantum tunneling in the resistance measurements. For the measurements in Fig. 8 the trigger level was 1 mV (compare with the  $V$ - $I$  curves in Fig. 6), but the results were essentially independent of the trigger level, for any reasonable choice. It is seen for all of the samples that at the highest temperatures (i.e., near  $T_c$ )  $I_s$  is fairly insensitive to the sweep speed, as would generally be found for a system with a "well-defined" critical current. However, for the large samples at the lowest temperatures one sees that  $I_s$  is a strong function of sweep speed. That is,  $\Gamma$  is a relatively slow function of  $I$ .

To check that the results in Fig. 8 were not due to some experimental artifact, the effects of shielding and isolation were again investigated, and did not appear to be a problem. Measurements of this kind were also performed with thin In films, such as the one considered in Fig. 2, and in that case  $I_s$  was essentially independent of sweep speed; i.e., the curves were almost exactly vertical in plots like those in Fig. 8. This all suggests that the behavior seen in Fig. 8 is not due to an experimental problem, such as extraneous noise. Indeed, the magnitude of outside noise would not change appreciably with temperature, and since the energy barrier is smallest near  $T_c$ , we would expect noise to have a much larger effect near  $T_c$ , and hence not lead to an appreciable variation far from  $T_c$  as found in Fig. 8. It seems safe to conclude that these results are not an experimental artifact. Further discussion of these results will be deferred to the next section, where we consider the theoretical predictions for the transition rates when  $I \lesssim I_c$ .

An important parameter in characterizing our system is the critical current. Since thermal activation and quantum tunneling both cause the system to switch to the normal state at currents below  $I_c$ , it is not possible to infer  $I_c$  simply from the  $V$ - $I$  measurements. However, in the limit of high sweep rates we expect that  $I_s \rightarrow I_c$ . Since the data in Fig. 8 indicate that  $I_s$  saturates in the limit of large  $dI/dt$ , these measurements can be used to determine  $I_c$ . Some typical results for  $I_c$  are shown in Fig. 9; these values were obtained by estimating the limiting value of  $I_s$  for large  $dI/dt$  from Fig. 8(a). GL theory predicts that  $I_c$  is related to the condensation energy, and hence the energy barrier according to<sup>36</sup>

$$I_c = \pi \left[ \frac{2}{3} \right]^{1/2} \frac{\Delta F_0}{\Phi_0/c} \sim \Delta T_c^{3/2}. \quad (5.1)$$

Measurements of  $I_c$  thus provide an independent check on the value of  $\Delta F_0$ . From (5.1), the theory predicts  $I_c \sim (T - T_c)^{3/2}$ , so in Fig. 9 we have plotted  $I_c^{2/3}$  as a function of  $T$ . The results for  $I_c$  are seen to be in good agreement with the predicted temperature dependence over essentially the entire range studied. This is consistent with previous studies of the range of validity of GL theory,<sup>51,52</sup> and indicates that the GL temperature

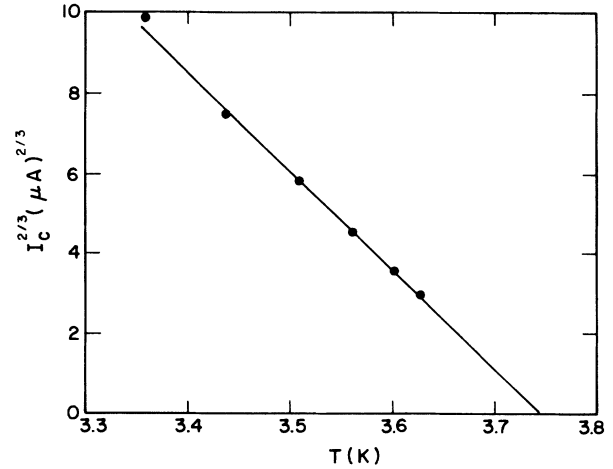


FIG. 9. Effective critical current, for a 640 Å sample, as a function of temperature. These results were derived from the data in Fig. 8(a), as described in the text. The straight line is a guide to the eye.

dependences for  $H_c$ ,  $\xi$ , and the other quantities discussed in this paper are accurate approximations over the range of temperature relevant here. The straight line through the data in Fig. 9 can be extrapolated to obtain an estimate of  $T_c$ . From Fig. 9 we find  $T_c \approx 3.743 \pm 0.010$  K, which compares favorably with the value  $T_c \approx 3.733 \pm 0.005$  K found for the codeposited film (and which was used to obtain the values in Table I).

The results for  $I_c$  can be used to estimate the magnitude of  $\Delta F_0$ , and thus provide a check on the value of  $\gamma_2$  obtained in the analysis of the resistance for  $I \rightarrow 0$ . When the results from Fig. 9 are expressed in terms of the dimensionless parameter  $\gamma_2$ , (4.1), we find  $\gamma_2 \approx 0.6$  for this sample. This is about a factor of 8 larger than the value found for this particular wire from the comparison of thermal activation theory with the resistance at low currents (sample 4 in Table I). The results for other samples showed somewhat closer agreement, with the difference being typically a factor of 2–4. The reason for this discrepancy is not entirely clear. It does *not* appear to be due to theoretical approximations. In particular, previous work<sup>51,52</sup> has demonstrated that the absolute magnitude predicted by the GL expression for  $I_c$ , (5.1), is accurate for samples of this size, and in this temperature range. The fact that the results for  $I_c$  indicate that  $\gamma_2 \approx 0.5$  for nearly all of our samples implies that the theory (5.1) works fairly well in this case, especially when we allow for uncertainties in  $H_c$ ,  $\xi$ , etc. As noted above, the value inferred for  $\gamma_2$  from the resistance measurements depends somewhat on the assumed value of  $T_c$ , and a relatively small reduction of  $T_c$  could easily increase  $\gamma_2$  by a factor of 2 or more, which would eliminate the discrepancy for most samples. Another possible reason for this discrepancy is the following. If a small amount of noise from higher temperatures reaches the samples, this would be manifest as an increased effective (i.e., noise) temperature, which would enter the denominator of the exponent of the thermal activation expression (4.1). This would lead to an erroneously small value

of  $\gamma_2$ . The noise temperature would have to be  $\approx 15$  K, and it is hard to rule out such an effect. Indeed, such behavior has been observed in previous work on tunnel junctions.<sup>41</sup> This would provide a natural explanation for the lower than expected values of  $\gamma_2$  in Table I. We should emphasize that the presence of this noise (if indeed this is the correct explanation of these observations) would *not* affect our conclusions concerning the importance of quantum tunneling, although it would, of course, affect the values of the parameters in Table I. Since we have concentrated on the *qualitative* behavior of the resistance (i.e., in Fig. 4), none of our conclusions concerning the interplay of thermal activation and quantum tunneling would be altered.

### B. Theory

An analysis of the results for  $I \lesssim I_c$  requires a consideration of how the thermal and quantum tunneling rates vary with  $I$ . The behavior of  $\Gamma_{TA}$  was worked out in detail by LA and MH. When the current is large, one need only consider transitions to states that lower  $\Delta\phi$ . This is in contrast to the situation for low currents [i.e., (3.9)] in which one must consider fluctuations that increase and decrease  $\Delta\phi$ . For transitions to the state of lower free energy one finds<sup>2,3</sup>

$$\Delta F_- = \frac{\sigma H_c^2 \xi}{8\pi} \left[ \frac{8\sqrt{2}}{3} (1-3\kappa^2)^{1/2} - 8\kappa(1-\kappa^2) \tan^{-1} \left[ \frac{(1-3\kappa^2)^{1/2}}{\sqrt{2}\kappa} \right] \right]. \quad (5.2)$$

The parameter  $\kappa$  was defined in (3.4), and is a function of  $I$ . When  $I \rightarrow I_c$ ,  $\kappa \rightarrow 1/\sqrt{3}$ . The corresponding attempt frequency is<sup>3</sup>

$$\Omega_- = \frac{\sqrt{3}L}{2\pi^{3/2}\xi\tau} (1-\sqrt{3}\kappa)^{15/4} (1+\kappa^2/4) (\Delta F_0/k_B T)^{1/2}, \quad (5.3)$$

which yields the thermal activation rate

$$\Gamma_{TA} = \Omega_- \exp(-\Delta F_-/k_B T). \quad (5.4)$$

Note that in the actual comparisons of the theory with our results we have inserted the parameters  $\gamma_1$  and  $\gamma_2$  in (5.4), in analogy with (4.1).

To obtain the quantum tunneling rate at finite currents it is necessary to generalize our previous results for the parameters  $A$  and  $B$  in (3.16) or the essentially equivalent (3.22). Given that our previous results for these parameters were only qualitative at best, we are now proceeding in a doubly qualitative manner. In the following we will use the language and results appropriate for the overdamped case, namely (3.17) and (3.19)–(3.22), although assuming that the system is underdamped would not yield any qualitative differences. [Note that MH theory (5.3) corresponds to thermal activation in the overdamped limit.] If we first consider  $B$ , (3.17), it is necessary to consider how the distance under the barrier  $\delta\phi$  varies as a function of  $I$ . Using the results of MH, the magnitude of the curvature at the top of the barrier is proportional to  $|\epsilon_{s1}|^{1/2}$ , where their parameter  $\epsilon_{s1}$  is given by

$$|\epsilon_{s1}| = \frac{1}{2} \{ [(1+\kappa^2)^2 + 3(1-3\kappa^2)^2]^{1/2} - (1+\kappa^2) \}. \quad (5.5)$$

The height of this barrier is  $\Delta F_-$ , which vanishes as  $I \rightarrow I_c$ . In this limit we would expect the shape of the potential to approach the form (3.20), and with this assumption the distance under the barrier is

$$\frac{\delta\phi}{(\delta\phi)_0} \approx \frac{1}{\sqrt{2}|\epsilon_{s1}|^{1/2}} \left[ \frac{\Delta F_-}{\Delta F_0} \right]^{1/2}, \quad (5.6)$$

where  $(\delta\phi)_0$  is the thickness of the barrier in the limit  $I \rightarrow 0$ . The factor  $\sqrt{2}$  in the denominator of (5.6) is needed for normalization, since  $|\epsilon_{s1}| \rightarrow \frac{1}{2}$  as  $I \rightarrow 0$ . The other parameter that enters  $B$ , (3.17), is  $\eta$ . This quantity follows directly from the equation of motion, (3.10); it does not depend on the shape of the potential, and hence should be independent of  $I$ .

We next consider the parameter  $A$ , (3.17). The arguments given in Sec. III implied that  $\alpha$  is a constant, and since it is a ratio of parameters that derive from the equation of motion, we expect it to remain unchanged. The barrier height that enters (3.17) is already known from  $\Delta F_-$ , (5.2). It then remains to estimate the frequency for small oscillations about the minima of the potential,  $\omega_0$ . For a potential of the form (3.20), the magnitude of the curvature at the bottom of the well is the same as that at the top of the barrier [e.g., (3.20)], which yields

$$\omega_0 \approx \tau^{-1} \sqrt{|\epsilon_{s1}|}. \quad (5.7)$$

TABLE I. Results for the parameters  $\gamma_1$ ,  $\gamma_2$ ,  $\beta_1$ , and  $\beta_2$ , obtained from comparisons with the theory, as in Figs. 4 and 5. Note that when  $\beta_1 = 0$  the results are independent of  $\beta_2$ , hence no value for  $\beta_2$  is listed in those cases.

| Sample | $\sigma^{1/2}$ (Å) | $\gamma_1$ | $\gamma_2$ | $\beta_1$ | $\beta_2$ |
|--------|--------------------|------------|------------|-----------|-----------|
| 1      | 410                | 1          | 0.22       | 0.003     | 0.055     |
| 2      | 420                | 1          | 0.43       | 0.006     | 0.035     |
| 3      | 485                | 3          | 0.18       | 0.003     | 0.05      |
| 4      | 640                | 0.03       | 0.07       | 0         |           |
| 5      | 745                | 0.03       | 0.035      | 0         |           |
| 6      | 1010               | 0.02       | 0.05       | 0         |           |

Collecting these results the quantum tunneling rate is given by (3.15) with

$$A = A_0 |\epsilon_{s1}|^{1/4} \left( \frac{\Delta F_-}{\Delta F_0} \right)^{1/2}, \quad B = B_0 \frac{\Delta F_-}{|\epsilon_{s1}| \Delta F_0}, \quad (5.8)$$

where  $A_0$  and  $B_0$  are the values of  $A$  and  $B$  in the limit  $I \rightarrow 0$ , from (3.22). When comparing this prediction with the experiments we will again insert the parameters  $\beta_1$  and  $\beta_2$ , as in (3.23).

### C. Comparison of theory and experiment

The next step is to compare the transition rates (5.4) and (5.8) with the results in Fig. 8. Given the highly qualitative nature of the model developed in the preceding section, we will consider if the *qualitative* features of the results can be accounted for by the model. With this in mind, we plot as the solid curves in Fig. 10 the prediction (5.4) for the thermal activation rate, while the dashed curves are the quantum tunneling theory, (5.8). The parameters  $\sigma$ , etc., are appropriate for the 640 Å sample considered in Fig. 8(a), and we have used the parameters  $\gamma_1 = 1$ ,  $\gamma_2 = 0.6$ ,  $\beta_1 = 0.003$ , and  $\beta_2 = 0.05$ . This value of  $\gamma_1$  amounts to using the theoretical prediction for  $\Omega_-$ . The value of  $\gamma_2$  was chosen to obtain agreement with the results for  $I_c$  (Fig. 9), while for  $\beta_1$  and  $\beta_2$  we have used the values obtained from the fits to the resistance, Table I.

From Fig. 10 we see that the transition rate predicted by the thermal activation model,  $\Gamma_{TA}$ , is a very strong function of  $I$ . It changes several decades for only a few percent change of  $I$ . We showed above that the results in Fig. 8 can be viewed as yielding the total transition rate  $\Gamma$  as a function of  $I$ , and hence the results in Fig. 10 can be compared directly with Fig. 8(a). We see that the variation of  $\Gamma_{TA}$  with  $I$  predicted by the thermal activation model is much faster than found in Fig. 8(a). For example, at  $T = 3.438$  K, the experiments show that for a 3 orders of magnitude change of  $\Gamma$ ,  $I$  changes by about

30%, while in Fig. 10 the change in  $I$  is *much* less. For *no* choice of parameters does the thermal activation prediction yield behavior even qualitatively similar to that seen experimentally.

From Fig. 10 we also see that the transition rate predicted by the quantum tunneling model  $\Gamma_{MQT}$  varies much more slowly with  $I$  than does  $\Gamma_{TA}$ . As discussed in Sec. V A, experimentally we have  $\Gamma \simeq (dI/dt)/\delta I_c$  in Fig. 8. Since  $\delta I_c \sim 0.01 I_c$  (see Fig. 7), the range of  $\Gamma$  probed in Fig. 8 corresponds to  $\Gamma \sim 1-10^3$ , which corresponds at least qualitatively with the calculated values. In this vicinity in Fig. 10 our model predicts a crossover from quantum tunneling at low currents to thermal activation at high currents. As with the behavior of the resistance in the limit  $I \rightarrow 0$  (Sec. IV), this cross-over can be traced to the different forms of the exponential factors in  $\Gamma_{TA}$ , and  $\Gamma_{MQT}$ . From Fig. 8 we see that this crossover is clearly observed in the experiments. At the lowest temperatures in Figs. 8(a) and (c) the slope of  $\Gamma \sim dI/dt$  is relatively small for low values of  $\Gamma$ , and becomes larger as  $\Gamma$  increases; this behavior is especially pronounced in the data at 3.438 and 3.359 K in Fig. 8(a). Hence we have a crossover from quantum tunneling to thermal activation as  $I$  increases. This crossover is predicted by the quantum tunneling model, Fig. 10, and the predictions are qualitatively consistent with the behavior seen experimentally.

The level of agreement between theory and experiment for  $\Gamma$  is much lower than was found in our analysis of the resistance at low currents. We have *not* attempted to adjust the parameters that enter  $\Gamma$  so as to obtain any kind of "best fit." Rather, we have chosen to emphasize the qualitative behavior of  $\Gamma$ . We have found that for any reasonable value of the parameters, the thermal activation transition rate,  $\Gamma_{TA}$ , is always a very strong function of  $I$ , and *never* shows the type of crossover behavior that is evident in the experimental results. For nearly all plausible parameter values the calculated transition rates show a crossover from quantum tunneling to thermal activation that is qualitatively very similar to that seen experimentally. We also note that according to the theory, for the smallest samples this crossover is predicted to occur at relatively small values of  $\Gamma$ , which is consistent with Fig. 8(b) where no crossover is seen in the experimentally accessible range.

While we have not performed any detailed fits, it seems likely that for some careful parameter choice(s) the model predictions for  $\Gamma$  could be made to agree quantitatively with the experiments. We have found that the value of  $\Gamma$  at which the crossover from thermal activation to quantum tunneling occurs can be varied by several orders of magnitude if the parameters  $\gamma_2$  and  $\beta_2$  are varied by reasonable amounts. However, such an exercise does not seem warranted, since the quantum tunneling model is at best only qualitative. The point we wish to emphasize again is that the thermal activation model alone cannot explain the experimental results. It is necessary to assume that there is some other mechanism for phase slip, and the quantum tunneling model is qualitatively consistent with the experimental observations.

It is useful to consider how the results for  $P(I)$  in Fig.

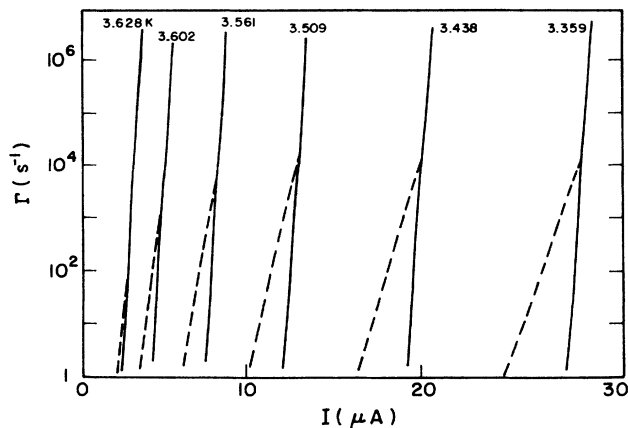


FIG. 10. Calculated transition rates for thermal activation (solid lines) and quantum tunneling (dashed lines). The parameters were appropriate for the 640 Å sample considered in Fig. 8(a), and are given in the text.

7, and those for  $\Gamma \sim dI/dt$  in Fig. 8 compare. We follow the recent discussion of Iansiti *et al.*<sup>50</sup> and assume for simplicity that the transition rate is dominated by a single exponential factor,

$$\Gamma(I_s) = \nu e^{-\Delta(I)}, \quad (5.9)$$

where  $\nu$  is the attempt frequency, and  $\Delta(I)$  is the appropriate normalized barrier height [for thermal activation  $\Delta(I)$  is the energy barrier normalized by  $k_B T$ ]. As discussed in Sec. VA, switching will occur when  $\Gamma(I_s)\delta I_c/(dI/dt) \sim 1$ , which yields<sup>50</sup>

$$I_s = I_c \left\{ 1 - \left[ \frac{1}{\Delta_0} \ln \left[ \frac{\nu \delta I_c}{dI/dt} \right] \right]^{1/\alpha} \right\}, \quad (5.10)$$

where  $\Delta(I) = \Delta_0(1 - I/I_c)^\alpha$ . It can also be shown that the width of the distribution is given by

$$\delta I_c = \alpha^{-1} \frac{I_c - I_s}{\ln[\nu \delta I_c/(dI/dt)]}. \quad (5.11)$$

Equations (5.10) and (5.11) imply that  $I_s$  and  $\delta I_c$  are, not surprisingly, related. If we choose a value of  $\Delta_0$  such that  $I_s/I_c \sim 0.5$ , a typical value in Fig. 8, we find from (5.10) and (5.11) that  $\delta I_c \sim 0.02I_c$ , which agrees with the results in Fig. 7 to within a factor of 2. We note that this requires  $\Delta_0 \sim 40$ , which seems reasonable based on our previous results, and we have used  $\alpha = \frac{3}{4}$  as appropriate here [see (5.2)]. Note also that this value of  $\delta I_c$  was used above to convert the values of  $dI/dt$  to  $\Gamma$  in our discussion of Fig. 8.

## VI. DISCUSSION

We have analyzed in detail the behavior of very thin In wires near the superconducting transition. Two types of measurements have been discussed. We first analyzed results for the resistance measured with small currents,  $I \ll I_c$ . For our largest samples it was only possible to obtain results relatively near  $T_c$ , while for the smaller samples the behavior could be studied over a fairly wide range. Near  $T_c$  the results for the resistance are in reasonable agreement with the thermal activation theory. However, at temperatures  $T_c - T \lesssim 0.2$  K the observed resistance cannot be explained by the thermal activation model. This suggests that there must be some other mechanism for phase slip in this region. We have shown that the behavior is consistent with a model based on quantum tunneling of the phase degree of freedom, similar to what has been observed in tunnel junctions and superconducting quantum-interference devices (SQUID's). The second type of measurement involves the behavior of the phase slip rate for currents near  $I_c$ . We have shown that these results cannot be explained by the thermal activation theory alone. The experiments again imply that there must be another mechanism for phase slip, and the quantum tunneling model is again qualitatively consistent with the experiments. It is noteworthy that the results for *both* our large and small samples indicate the presence of a phase-slip mechanism in addition to thermal activation. In order to interpret our results we have developed

a qualitative model of quantum phase slip, based on analogies with the theory of macroscopic quantum tunneling. At present this analogy is incomplete, due to uncertainties in the equation of motion appropriate for our case. A quantitative theoretical study of this question would be most welcome.

So far as we know, the only previous experiments that have been aimed at observing quantum tunneling in one-dimensional superconductors are those of Mooij and co-workers.<sup>8</sup> They interpreted their results in terms of the thermal activation model, and reported reasonable agreement. However, their samples were somewhat wider than ours (typically by a factor of 10), and were one dimensional only fairly near  $T_c$ . It would be interesting to make a detailed comparison of the results of Mooij and co-workers and the quantum tunneling model.

In conclusion, we again wish to emphasize that our results certainly do *not* rule out the possibility that the behavior we have observed is due to some hitherto unidentified phase-slip mechanism, other than quantum tunneling. However, it does appear that all of our results are consistent with the quantum tunneling model. It will be interesting to see if any related quantum effects can be observed in this system.

## ACKNOWLEDGMENTS

I thank P. Muzikar for many stimulating and critical discussions, R. Landauer, A. J. Leggett, T. R. Lemberger, T. L. Meisenheimer, and A. W. Overhauser for some very helpful comments and correspondence, and E. Sweetland for invaluable assistance with the fabrication. This work was supported by the National Science Foundation through Grant No. DMR-8614862.

## APPENDIX

Here we consider the values of the parameters  $\gamma_1$ ,  $\gamma_2$ ,  $\beta_1$ , and  $\beta_2$  from Table I. To this point in our analysis we have not placed much emphasis on the precise numerical values of these parameters, concentrating instead on the qualitative form of the quantum tunneling rate. Our rationale has been that this theory is extremely qualitative, and hence that the numerical factors should not be taken too seriously. Nevertheless, it is interesting to consider these values in a little more detail.

We first consider  $\gamma_1$  and  $\gamma_2$ . These parameters multiply, respectively, the attempt frequency and free-energy barrier in the expression for the thermal activation rate, (4.1). If the LA-MH theory worked perfectly and our estimates of parameters such as  $T_c$ ,  $H_c$ , etc., were all accurate, then  $\gamma_1$  and  $\gamma_2$  would both be unity. We see from Table I that this is not the case. The theoretical predictions are much more sensitive to  $\gamma_2$  since it multiplies the exponent. Variations of the prefactor  $\gamma_1$  by a factor of 10 or more can be compensated for by relatively small changes in  $\gamma_2$ . In addition, in previous comparisons with the thermal activation theory<sup>4-7</sup> reductions of the prefactor by a factor of 10 or more were sometimes required. Finally, as we noted above, phase slip will occur preferentially at the locations at which the cross-sectional area is smallest, and that if there are only a few such places the

value of the thermal activation attempt frequency will be significantly reduced. This would be manifest as a value of  $\gamma_1$  less than unity. Thus, there are several ways to account for the observed values of  $\gamma_1$ .

The values of  $\gamma_2$  in Table I are also seen to be less than unity. As discussed above, an independent estimate of  $\gamma_2$  can be obtained from the value of the critical current. For the 640 Å wire considered in Fig. 9, the value of  $\gamma_2$  obtained from  $I_c$  was  $\approx 0.6$ , which is about a factor of 8 larger than inferred from the analysis of the resistance. For other samples the difference was not as large. For the 410 Å sample the  $I_c$  data yielded  $\gamma_2 = 0.4$  while the resistance data gave  $\gamma_2 = 0.22$  (Table I), while for the 1010 Å sample the two values were 0.2 and 0.05, respectively. This difference could arise in several different ways. First, as noted above, a small amount of external noise could lead to an effective (noise) temperature above the ambient temperature, and this would act to depress the value of  $\gamma_2$ . A noise temperature of order 15 K would be required, and it is difficult to rule out such an effect. Note that even if this noise were present, none of our conclusions concerning the failure of thermal activation theory, or the relevance of quantum tunneling would be affected. Another way to account for this discrepancy would be an error in the choice of  $T_c$  in the analysis of the resistance data. As noted above, we used the value of  $T_c$  measured for co-deposited films. However, it is possible that this is not the proper value. Theoretical work<sup>53</sup> predicts that the presence of disorder should have a significant dimensionality dependent effect on  $T_c$ . For

our one-dimensional samples, the theory predicts a suppression of  $T_c$  much too large to be consistent with our results.<sup>34,54</sup> However, it is possible that this mechanism could cause a relatively small downward shift of  $T_c$  for the wires, and this would reduce the value of  $\gamma_2$  inferred from the resistance data. Rough estimates indicate that this could cause a factor of 2 (or more) change in  $\gamma_2$ . Hence, most of the discrepancy could be accounted for in this way. Again, we emphasize that this would in no way affect the conclusions we have drawn in this paper.

Let us now consider the values of  $\beta_1$  and  $\beta_2$ . In our development of the quantum tunneling model, we ignored numerous factors of order unity. We expected  $\beta_1$  and  $\beta_2$  to be of order unity, and it seen from Table I that they are both somewhat smaller than this. We will first assume that the overdamped limit is appropriate, hence we will begin by using (3.22). Comparing (3.23) with (3.22) one finds that if all of the numerical factors in (3.22) are correct (which we certainly do not claim to be the case), then  $\beta_1$  should be equal to  $8\sqrt{2}/(36\sqrt{2})^{7/2} \approx 1.2 \times 10^{-5}$ , which is much smaller than the experimental values (Table I). If we use the result for weak damping, (3.16), we find  $\beta_1 \approx 4.7$ . Presumably for intermediate damping  $\beta_1$  would lie between these two values, which would be consistent with the values in Table I. Thus the observed values of  $\beta_1$  seem quite reasonable. Turning to  $\beta_2$  we see from (3.22) that (again assuming this expression is accurate)  $\beta_2 = \pi/(6\sqrt{2}) \approx 0.37$ , which is reasonably close to the values found in Table I. Hence, the experimental values again appear to be reasonable.

<sup>1</sup>W. A. Little, Phys. Rev. **156**, 396 (1967).

<sup>2</sup>J. S. Langer and V. Ambegaokar, Phys. Rev. **164**, 498 (1967).

<sup>3</sup>D. E. McCumber and B. I. Halperin, Phys. Rev. B **1**, 1054 (1970).

<sup>4</sup>J. E. Lukens, R. J. Warburton, and W. W. Webb, Phys. Rev. Lett. **25**, 1180 (1970).

<sup>5</sup>R. S. Newbower, M. R. Beasley, and M. Tinkham, Phys. Rev. B **5**, 864 (1972).

<sup>6</sup>J. R. Miller and J. M. Pierce, Phys. Rev. B **8**, 4164 (1973); *Proceedings of the 13th International Conference on Low Temperature Physics, Boulder, 1972*, edited by W. S. O'Sullivan (Plenum, New York, 1974), Vol. III, p. 659.

<sup>7</sup>For a review, see W. J. Skocpol and M. Tinkham, Rep. Prog. Phys. **38**, 1049 (1975).

<sup>8</sup>A. J. Van Run, J. Romijn, and J. E. Mooij, Jpn. J. Appl. Phys. **26**, Pt. 1, 1765 (1987).

<sup>9</sup>J. Kurkijärvi, in *SQUID-80: Superconducting Quantum Interference Devices and Their Applications*, edited by H. D. Hahlbohm and H. Lubbig (de Gruyter, Berlin, 1980), p. 247.

<sup>10</sup>A. O. Caldeira and A. J. Leggett, Phys. Rev. Lett. **46**, 211 (1981); Ann. Phys. (N.Y.) **149**, 374 (1983).

<sup>11</sup>Preliminary reports of some of our results have been given in Refs. 12 and 13.

<sup>12</sup>N. Giordano, Phys. Rev. Lett. **61**, 2137 (1988).

<sup>13</sup>N. Giordano, in *Proceedings of the International Symposium on Nanostructure Physics and Fabrication*, edited by W. P. Kirk and M. A. Reed (Academic, San Diego, 1989), p. 473.

<sup>14</sup>D. E. Prober, M. D. Feuer, and N. Giordano, Appl. Phys.

Let. **37**, 94 (1980).

<sup>15</sup>N. Giordano, Phys. Rev. B **22**, 5635 (1980).

<sup>16</sup>See, for example, W. J. Skocpol, PhD. thesis, Harvard University, 1974 (unpublished).

<sup>17</sup>Keithley model 195 and Data Precision model 3600 digital voltmeters were used.

<sup>18</sup>Princeton Applied Research model 113.

<sup>19</sup>M. Cyrot, Rep. Prog. Phys. **36**, 103 (1973).

<sup>20</sup>A. Barone and G. Paterno, *Physics and Applications of the Josephson Effect* (Wiley, New York, 1982).

<sup>21</sup>If one considers the full-current dependence of the transition rate, one finds for low currents that the voltage is proportional to  $\sinh(I)$ . As  $I \rightarrow 0$  this factor is proportional to  $I$ , and hence the predicted resistance is independent of  $I$ .

<sup>22</sup>R. Landauer and J. A. Swanson, Phys. Rev. **121**, 1668 (1961).

<sup>23</sup>S. Saito and Y. Murayama, Phys. Lett. A **135**, 55 (1989).

<sup>24</sup>V. Ambegaokar, U. Eckern, and G. Schön, Phys. Rev. Lett. **48**, 1745 (1982).

<sup>25</sup>P. Hänggi, J. Stat. Phys. **42**, 105 (1986).

<sup>26</sup>A. J. Leggett, S. Chakravarty, A. T. Dorsey, M. P. A. Fisher, A. Garg, and W. Zwerger, Rev. Mod. Phys. **59**, 1 (1987).

<sup>27</sup>Here we ignore effects such as the thermal enhancement of the quantum tunneling rate, as they appear to be small compared to the main temperature dependence arising from that of  $\exp(-B)$ .

<sup>28</sup>A. I. Larkin and Yu. N. Ovchinnikov, Zh. Eksp. Teor. Fiz. **86**, 719 (1984) [Sov. Phys.—JETP **59**, 420 (1984)].

<sup>29</sup>H. Grabert, P. Olschowski, and U. Weiss, Phys. Rev. B **32**,

- 3348 (1985).
- <sup>30</sup>See, for example, J. E. Mooij and G. Schön, *Phys. Rev. Lett.* **55**, 114 (1985).
- <sup>31</sup>In addition, for  $T \approx 0$  the time dependent GL equation does yield a mass-like term (see, e.g., Ref. 23).
- <sup>32</sup>The extra terms in the prefactor in (3.24) arise in the following way. The voltage is proportional to the sum of the rates of two processes, one which increases  $I$ , and one that decreases  $I$ . The two processes have nearly the same energy barrier, the only difference being due to (3.7). When one adds the two rates, and then takes the limit  $I \rightarrow 0$ , the extra factors in (3.24) appear. This is completely analogous to the derivation of (3.13); see Ref. 2.
- <sup>33</sup>See, for example, B. I. Belevtsev, V. V. Pilipenko, and L. A. Yatsuk, *Fiz. Nizk. Temp.* **7**, 1010 (1981) [*Sov. J. Low Temp. Phys.* **7**, 490 (1981)].
- <sup>34</sup>For additional discussion of the behavior of  $T_c$  of the In films, see N. Giordano and E. Sweetland, *Phys. Rev. B* **39**, 6455 (1989).
- <sup>35</sup>The measurements shown in Figs. 2–5 were all performed at currents sufficiently small that the resistance was independent of the current; i.e., the voltage was a linear function of the current. Currents typically as small as  $\sim 3 \times 10^{-10}$  A were used, while the largest current that could be used, while staying in the linear regime, depended on the size of the wire. This largest current was typically  $\lesssim 1 \times 10^{-7}$  A for our smallest samples, and about a factor of 10 larger for the largest samples.
- <sup>36</sup>See, for example, M. Tinkham, *Introduction to Superconductivity* (McGraw-Hill, New York, 1975).
- <sup>37</sup>We used  $H_c(T=0) = 286$  Oe [see R. W. Shaw, D. E. Mapother, and D. C. Hopkins, *Phys. Rev.* **120**, 88 (1960)]. The coherence length was estimated from the standard relation (see Ref. 36)  $\xi(T=0) = 0.86\sqrt{\lambda\xi_0}$ , where for In  $\xi_0 = 2.6 \times 10^{-5}$  cm [see A. M. Toxen, *Phys. Rev.* **123**, 442 (1961)] and  $\lambda$  is the mean free path.  $\lambda$  was estimated from the resistivity and the measured  $\rho\lambda$  product [ $\rho\lambda = 1.1 \times 10^{-11}$   $\Omega$  cm<sup>2</sup>, K. R. Lyall and J. F. Cochran, *Phys. Rev.* **139**, 517 (1967)]. The mean free path was 240 Å for the largest samples, and 95 Å for the smallest samples.
- <sup>38</sup>As discussed in Ref. 34, theory predicts that the disorder present in our samples should lead to a rather large shift of  $T_c$  relative to the value found for either bulk material or films of comparable thickness. It is shown in Ref. 34 that this shift is actually very small, and in our analysis we have assumed that it is negligible. However, it is possible that this shift is not insignificant. This shift of  $T_c$ , which would be size dependent, could lead to the behavior of  $\gamma_2$  seen in Table I.
- <sup>39</sup>The parameter  $\gamma_2$  adjusts the value of the energy barrier  $\Delta F_0$  to provide a best fit to the results in the thermal activation regime. The intent here is that  $\gamma_2$  corrects  $\Delta F_0$  for uncertainties in our estimates of  $H_c$ , etc. We have therefore used this corrected value of  $\Delta F_0$  in evaluating the resistance due to quantum tunneling (3.24). That is, everywhere  $\Delta F_0$  appears in (3.24) we have replaced it with  $\gamma_2\Delta F_0$ .
- <sup>40</sup>L. D. Jackel, W. W. Webb, J. E. Lukens, and S. S. Pei, *Phys. Rev. B* **9**, 115 (1974).
- <sup>41</sup>T. A. Fulton and L. N. Dunkleberger, *Phys. Rev. B* **9**, 4760 (1974).
- <sup>42</sup>R. F. Voss and R. A. Webb, *Phys. Rev. Lett.* **47**, 265 (1981).
- <sup>43</sup>L. D. Jackel, J. P. Gordon, E. L. Hu, R. E. Howard, L. A. Fetter, D. M. Tennant, R. W. Epworth, and J. Kurkijärvi, *Phys. Rev. Lett.* **47**, 697 (1981).
- <sup>44</sup>S. Washburn, R. A. Webb, R. F. Voss, and S. M. Faris, *Phys. Rev. Lett.* **54**, 2712 (1985).
- <sup>45</sup>D. B. Schwartz, B. Sen, C. N. Archie, and J. E. Lukens, *Phys. Rev. Lett.* **55**, 1547 (1985).
- <sup>46</sup>M. H. Devoret, J. M. Martinis, and J. Clarke, *Phys. Rev. Lett.* **55**, 1908 (1985).
- <sup>47</sup>J. M. Martinis, M. H. Devoret, and J. Clarke, *Phys. Rev. B* **35**, 4682 (1987).
- <sup>48</sup>N. Giordano, W. Gilson, and D. E. Prober, *Phys. Rev. Lett.* **43**, 725 (1979); J. T. Masden and N. Giordano, *ibid.* **49**, 819 (1982); J. J. Lin and N. Giordano, *Phys. Rev. B* **35**, 545 (1987).
- <sup>49</sup>The  $V$ - $I$  curves in Fig. 6 are qualitatively similar to what one might expect from a “thermal runaway” type of behavior. However, we also performed measurements in which the current was quickly set to a value near the onset of the  $V$ - $I$  curve, and then monitored the voltage as a function of time. For values of  $I$  just at the onset the voltage increased very slowly, with a time constant as large as 10 min or more, and it was not clear that the voltage would ever reach a value corresponding to the normal state. It is hard to see how this could be due to thermal runaway, and we therefore do not believe that this phenomenon played an important role here.
- <sup>50</sup>M. Iansiti, M. Tinkham, A. T. Johnson, W. F. Smith, and C. J. Lobb, *Phys. Rev. B* **39**, 6465 (1989).
- <sup>51</sup>J. Romijn, T. M. Klapwijk, M. J. Renne, and J. E. Mooij, *Phys. Rev. B* **26**, 3648 (1982).
- <sup>52</sup>W. J. Skocpol, *Phys. Rev. B* **14**, 1045 (1976).
- <sup>53</sup>H. Ebisawa, H. Fukuyama, and S. Maekawa, *J. Phys. Soc. Jpn.* **55**, 4408 (1986).
- <sup>54</sup>In Ref. 34 we obtained an approximate value of  $T_c$  from the midpoint of the resistive transition. A more complete analysis in terms of the thermal activation model, etc., would of course yield a higher value of  $T_c$ . However, for the purposes of Ref. 34 this rough estimate was sufficient.